Available online at www.sciencedirect.com
ScienceDirect
Journal of Solid State Chemistry 180 (2007) 313–321
JOURNAL OF SOLID STATE CHEMISTRY
www.elsevier.com/locate/jssc

Structure and electron density analysis of electrochemically and chemically delithiated $LiCoO_2$ single crystals

Yasuhiko Takahashi[a], Norihito Kijima[a], Kaoru Dokko[b,1], Matsuhiko Nishizawa[b], Isamu Uchida[b], Junji Akimoto[a,*]

[a]*National Institute of Advanced Industrial Science and Technology (AIST), 1-1-1 Higashi, Tsukuba 305-8565, Japan*
[b]*Graduate School of Engineering, Tohoku University, Aramaki-Aoba, Aoba-ku, Sendai 980-8579, Japan*

Received 13 July 2006; received in revised form 11 October 2006; accepted 12 October 2006
Available online 29 October 2006

Abstract

Single crystals of $Li_{0.68}CoO_2$, $Li_{0.48}CoO_2$, and $Li_{0.35}CoO_2$ were successfully synthesized for the first time by means of electrochemical and chemical delithiation processes using $LiCoO_2$ single crystals as a parent compound. A single-crystal X-ray diffraction study confirmed the trigonal $R\bar{3}m$ space group and the hexagonal lattice parameters $a = 2.8107(5)$ Å, $c = 14.2235(6)$ Å, and $c/a = 5.060$ for $Li_{0.68}CoO_2$; $a = 2.8090(15)$ Å, $c = 14.3890(17)$ Å, and $c/a = 5.122$ for $Li_{0.48}CoO_2$; and $a = 2.8070(12)$ Å, $c = 14.4359(14)$ Å, and $c/a = 5.143$ for $Li_{0.35}CoO_2$. The crystal structures were refined to the conventional values $R = 1.99\%$ and $wR = 1.88\%$ for $Li_{0.68}CoO_2$; $R = 2.40\%$ and $wR = 2.58\%$ for $Li_{0.48}CoO_2$; and $R = 2.63\%$ and $wR = 2.56\%$ for $Li_{0.35}CoO_2$. The oxygen–oxygen contact distance in the CoO_6 octahedron was determined to be shortened by the delithiation from 2.6180(9) Å in $LiCoO_2$ to 2.5385(15) Å in $Li_{0.35}CoO_2$. The electron density distributions of these Li_xCoO_2 crystals were analyzed by the maximum entropy method (MEM) using the present single-crystal X-ray diffraction data at 300 K. From the results of the single-crystal MEM, strong covalent bonding was clearly visible between the Co and O atoms, while no bonding was found around the Li atoms in these compounds. The gradual decrease in the electron density at the Li site upon delithiation could be precisely analyzed.

Keywords: Crystal structure; $LiCoO_2$; Li_xCoO_2; Single-crystal X-ray diffraction; Electron density analysis; MEM

1. Introduction

Lithium cobalt dioxide, $LiCoO_2$, has a trigonal α-$NaFeO_2$ structure and has been the most widely used positive electrode material in commercial secondary lithium-ion batteries for over the 10 years due to its easy preparation, high theoretical specific capacity, and other advantages.

The crystal and electronic structural changes upon delithiation in $LiCoO_2$ have been extensively studied by means of various experimental [1–13] and theoretical techniques [14–18], for they are believed to influence the reversibility of the charge–discharge process in batteries.

Based on the previous structural works [3–8], the phase changes upon delithiation in Li_xCoO_2 ($0.35 < x < 1$) have been confirmed as follows: trigonal I in the compositional range of $0.94 < x < 1$; trigonal I + trigonal II in $0.75 < x < 0.94$; trigonal II in $0.5 < x < 0.75$; monoclinic in $x = 0.5$; and trigonal II in $0.35 < x < 0.5$. In particular, the existence of a two-phase region corresponding to a voltage plateau for $0.75 < x < 0.94$ in Li_xCoO_2 [19,20] and the presence of a monoclinic symmetry for $x = 0.5$ attributed to a lithium/vacancy ordering [21,22] have been extensively investigated. However, detailed structural changes, i.e., the bond distance and displacement parameter of atoms upon delithiation, are not clearly understood yet.

In $LiCoO_2$, it has traditionally been accepted that the valence state of the Co atom compensates for the charge upon the Li^+ deintercalation. The assumption is that the oxygen valence is fixed to O^{2-}, so the charge compensation upon delithiation occurs at the Co atoms; that is, the Co

*Corresponding author. Fax: +81 29 861 9214.
E-mail address: j.akimoto@aist.go.jp (J. Akimoto).
[1]Present address: Department of Applied Chemistry, Tokyo Metropolitan University, 1-1 Minami-Ohsawa, Hachioji, Tokyo 192-0397, Japan.

0022-4596/$ - see front matter © 2006 Elsevier Inc. All rights reserved.
doi:10.1016/j.jssc.2006.10.018

valence changes from Co^{3+} to Co^{4+} upon delithiation. On the other hand, recent theoretical calculations on the electronic structure changes upon delithiation have shown that the oxygen valence plays a dominant role in accepting the incoming charge [15,17,18]. A similar feature has been confirmed by experimental approaches using X-ray absorption spectroscopy (XAS) [9–11] and electron energy-loss spectroscopy (EELS) [12].

To clarify the physical and chemical properties, it is important to understand the nature of chemical bonding in detail. The accurate single-crystal X-ray diffraction study is one of the most effective methods for precisely understanding the nature of bonding, the interatomic distances, and the thermal displacement parameters of atoms in materials. In addition, in the past few years, a new method, the maximum entropy method (MEM), has been found to be efficient for determining their electron density distributions in crystalline materials [23–25]. There have been many theoretical electron density studies of the delithiated Li_xCoO_2 [16–18]; to our knowledge, however, there has been no experimental electron density analysis of Li_xCoO_2.

We recently synthesized $LiCoO_2$ single crystals by a flux method, and revealed the precise structural and physical properties [26,27]. In addition, electrochemical delithiation experiments using $LiCoO_2$ single crystals have been carried out by a microelectrode-based characterization system [28]. In the present study, we report the experimental details for electrochemical and chemical delithiation using single crystal specimens, and the structure refinements of three delithiated compounds, $Li_{0.68}CoO_2$, $Li_{0.48}CoO_2$, and $Li_{0.35}CoO_2$, using single-crystal X-ray diffraction data.

2. Experimental

2.1. Single crystal synthesis

Single crystals of $LiCoO_2$ were grown by a flux method, as mentioned previously [26,27]. The as-prepared $LiCoO_2$ powder (Cell Seed C; Nippon Chemical Industrial Co., Ltd., Tokyo, Japan) was mixed with Li_2O_2 (99.9%) and LiCl (99.9%) to form flux material in the nominal weight ratio of $LiCoO_2$: Li_2O_2: LiCl = 1: 4: 4. The mixture was heated at 1173 K for 10 h in a sealed gold tube, gradually cooled to 873 K at a rate of 5 K/h, and then cooled naturally. The produced single crystals were easily separated from the frozen flux by rinsing the gold tube in water for several minutes. Black, hexagonal platelet single crystals of about $0.1 \times 0.1 \times 0.01\,mm^3$ in average were obtained, as reported previously [26,27]. The crystals thus obtained were investigated by scanning electron microscopy-energy dispersive X-ray analysis (SEM-EDX; JEOL JSM-5400) and inductively coupled plasma-atomic emission spectroscopy (ICP-AES; Perkin Elmer, Inc., Optima 3000). EDX analysis showed that the as-grown crystals were free from gold contamination from the crucible. The chemical composition was analyzed by ICP-AES and determined to be Li: Co: O=1.0: 1.0: 2, which is consistent with the previous results [27]. It should be noted that single crystals of the recently reported "lithium overstoichiometric" $Li_{1.1}CoO_2$ [29–31] could not be synthesized in the present study.

2.2. Electrochemical delithiation

The controlled extraction of Li-ions from a piece of single crystal was achieved by electrochemical means using a microelectrode-based system [25,32–35]. A selected $LiCoO_2$ crystal was placed on a glass paper soaked in 1 M $LiClO_4$/propylene carbonate (PC) + ethylene carbonate (EC) (1:1 in volume) solution (Li-ion battery grade; Mitsubishi Kagaku Co.). A Pt–Rh fine filament (25 μm in diameter) was coated with a thin film of Teflon (Cytop; Asahi Glass), then cut to give a micro-disk electrode. The prepared microelectrode was held with an x–y–z micropositioner (Shimadzu MMS-77) and brought into contact with the $LiCoO_2$ crystal by handling the positioner under observation with a stereomicroscope (Nikon SMZ-U). The electrode potential was measured and controlled against a Li foil reference electrode with a potentiostat (Hokuto Denko HA-150). All the electrochemical experiments were conducted in a small dry box filled with air purified by a column (Balston 75-20; 203 K dew point).

The microelectrode was brought closer to the large hexagonal crystal face. At the moment of contact, the open circuit potential (OCP) changed suddenly from a value around 3.1 V to 3.5 V vs. Li, reflecting the OCP of $LiCoO_2$. At first, the cyclic voltammograms using a small $LiCoO_2$ single crystal ($25 \times 25 \times 12\,\mu m^3$) were recorded to reveal the Li-ion deintercalation–intercalation reactions. The CV of a $LiCoO_2$ single crystal at a scan rate of 0.1 mV/s is shown in Fig. 1. A sharp current peak can be seen at 4.1 V during the first anodic scan, and a broad peak around 3.9 V during cathodic scan. This fact indicated that the present electrochemical technique was useful to control the lithium content in the $LiCoO_2$ single crystal specimens. However, at 2nd cycle, the anodic peak shifted to 4.25 V, and the cathodic current became smaller. These facts indicated that the Li-ion deintercalation and intercalation into the $LiCoO_2$ single crystal did not process reversibly. Further experiments should be performed to reveal the bulk electrochemical properties using the single crystal specimens.

In the present study, the electrode potential of the larger single crystals having 100–500 μm sizes was controlled by stepping-up from the OCP to the desired values of 3.92 and 4.12 V vs. Li. Anodic current at the level of a few mA was observed due to the Li^+ extraction from the crystal. After overnight electrolysis, the potentiostat was switched back to the OCP-measuring mode. We checked the completion of the extraction reaction with the stability of the regulated OCP. When the reaction was not complete, the OCP value shifted back to a negative value. The obtained Li_xCoO_2 crystal was rinsed carefully with pure PC, and then subjected to the single-crystal X-ray diffraction analysis.

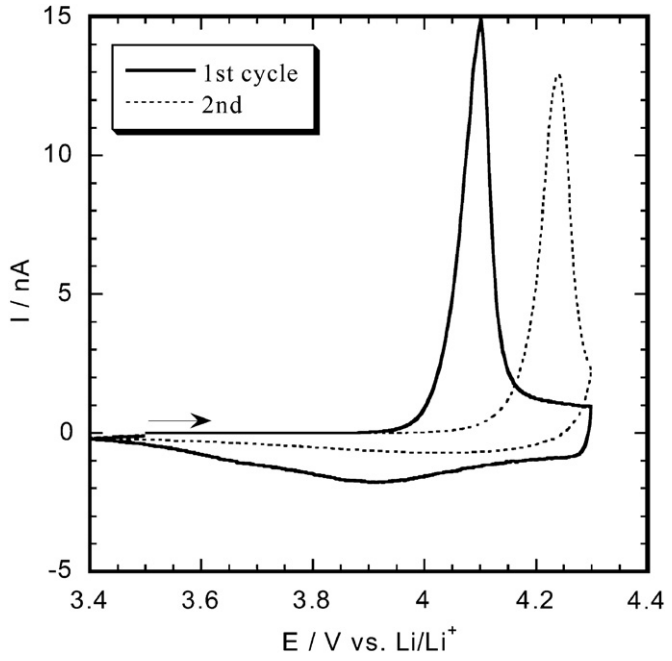

Fig. 1. Cyclic voltammograms of a $LiCoO_2$ single crystal in 1 M $LiClO_4$/PC + EC at a scan rate of 0.1 mV/s.

We succeeded in the electrochemical preparation of the two Li-deficient single crystal specimens in this study, $Li_{0.68}CoO_2$ (3.92 V vs. Li) and $Li_{0.48}CoO_2$ (4.12 V vs. Li). The reproducibility of the chemical composition and structural parameters in the electrochemical preparation for Li_xCoO_2 single crystals has been checked by structure analysis using two Li_xCoO_2 specimens at 3.92 V. Their lattice parameters, structural parameters and lithium occupancy parameters were within their estimated standard deviations. The chemical formulae of these oxidized crystals were determined by the present single-crystal X-ray structure analyses.

2.3. Chemical delithiation

The Li_xCoO_2 single crystals were also prepared by a combined Li-ion extraction/chemical oxidation process. Selected $LiCoO_2$ single crystals were placed in 1 M HCl solution for several days. No stirring or heating was performed. The bubbling of H_2 gas from the surface regions of crystals was observed. This fact suggested the production of the Li deficient single crystals due to the reaction

$$2\,LiCoO_2 + 2(1-x)\,H^+ \rightarrow 2\,Li_xCoO_2 + 2(1-x)\,Li^+ + (1-x)\,H_2\uparrow .$$

The obtained Li_xCoO_2 crystal was carefully washed with ethanol, and then subjected to the single-crystal X-ray diffraction analysis. We succeeded in the chemical preparation of the two Li-deficient single crystal specimens in this study, $Li_{0.52}CoO_2$ (reaction time: 2 days) and $Li_{0.35}CoO_2$ (7 days). The chemical formulae of these oxidized crystals were determined by the present single-crystal X-ray structure analyses. The lattice constants and structural parameters for the chemically delithiated $Li_{0.52}CoO_2$ were in good agreement with those for the above-mentioned electrochemically delithiated $Li_{0.48}CoO_2$.

It should be noted that the bubbling of H_2 gas from the surface regions of the $LiCoO_2$ crystals was observed in the present chemical delithiation process, as mentioned above. This fact strongly suggested the production of the delithiated single crystals, not lithium/proton exchanged samples. In addition, the c-axis length (13.150(5) Å) for the isostructural protonated compound $HCoO_2$ [36] is much shorter than that (14.0536(5) Å) for $LiCoO_2$ [26]. On the contrary, the a-axis length (2.851(1) Å) for $HCoO_2$ is much longer than that (2.8161(5) Å) for $LiCoO_2$. Therefore, if the acid-treated crystal has the chemical composition such as $Li_xH_{1-x}CoO_2$, the a-axis should increase and the c-axis should decrease upon ion-exchange reaction. However, the present chemical delithiation experiments show that the a-axis length decreases and the c-axis increases drastically upon delithiation. Furthermore, the lattice parameter change by the chemical method is in good agreement with that by the present electrochemical method, as mentioned later. For these reasons, we believe that the lithium/proton ion exchange reaction could not proceed preferentially in the present experiments.

2.4. Single-crystal X-ray diffraction

Four crystals of Li_xCoO_2 with $x = 1$, 0.68, 0.48 and 0.35 were mounted on glass fibers for single-crystal X-ray diffraction studies. The crystals were examined with an X-ray precession camera (Mo$K\alpha$ radiation) in order to check the crystal quality and to determine the lattice parameters, systematic extinctions, and possible superstructures. The single-crystallinity changes upon delithiation for the Li_xCoO_2 single crystals were checked using peak profiles of the main reflections examining the ω-scan mode with a step scan interval of 0.05° and a counting time of 1 s. The hexagonal lattice parameters of the Li_xCoO_2 single crystals, determined by least-squares refinement using 2θ values of 25 strong reflections in the range 50–70° and Mo$K\alpha_1$ ($\lambda = 0.70926$ Å) on a Rigaku AFC-5S four-circle diffractometer, are listed in Table 1.

Integrated intensity data for the as-grown $LiCoO_2$ and the delithiated Li_xCoO_2 single crystals were collected in the $2\theta - \omega$ scan mode at a scan rate of 1°/min at 300 K on the four-circle diffractometer (operating conditions: 45 kV, 35 mA) using graphite-monochromatized Mo$K\alpha$ radiation ($\lambda = 0.71073$ Å), and reduced to structure factors after due corrections for absorption and Lorentz and polarization effects. The structure refinement was carried out with the atomic coordinates of $LiCoO_2$ ($R\bar{3}m$ space group; Li at the 3a site, Co at the 3b site and O at the 6c site) [26]. The lithium site occupancy value was refined in the calculations. The converged final R and wR values and

Table 1
Crystallographic and experimental summary for Li_xCoO_2

Composition	$LiCoO_2$	$Li_{0.68}CoO_2$	$Li_{0.48}CoO_2$	$Li_{0.35}CoO_2$
Space group	$R\bar{3}m$	$R\bar{3}m$	$R\bar{3}m$	$R\bar{3}m$
Lattice parameters				
a (Å)	2.8156(6)	2.8107(5)	2.8090(15)	2.8070(12)
c (Å)	14.0542(6)	14.2235(6)	14.3890(17)	14.4359(14)
V (Å^3)	96.49(4)	97.31(3)	98.33(11)	98.51(8)
D_x (g/cm^3)	5.053	4.889	4.776	4.721
Crystal size (μm)	120 × 100 × 10	100 × 100 × 10	460 × 140 × 60	160 × 70 × 10
Temperature (K)	300	300	300	300
Maximum 2θ (deg)	130	130	130	135
Transmission factors				
Min.	0.320	0.352	0.097	0.340
Max.	0.872	0.869	0.500	0.943
Measured reflections	2236	2228	2286	1958
R_{int}	2.01%	2.14%	2.89%	3.65%
Independent reflections	250	252	256	262
Number of variables	9	10	10	10
R	2.01%	1.99%	2.40%	2.63%
wR [$w = 1/\sigma^2 F$]	2.09%	1.88%	2.58%	2.56%

Table 2
Atomic coordinates, displacement parameters,[a] and site occupancy factors for Li_xCoO_2

		$LiCoO_2$	$Li_{0.68}CoO_2$	$Li_{0.48}CoO_2$	$Li_{0.35}CoO_2$
Li	x	0	0	0	0
	y	0	0	0	0
	z	0	0	0	0
	U_{eq}	0.012(2)	0.017(3)	0.023(7)	0.028(10)
	U_{11}	0.0126(14)	0.021(3)	0.030(8)	0.038(11)
	U_{33}	0.011(2)	0.009(3)	0.009(5)	0.009(9)
	s.o.f.	1	0.68(3)	0.48(6)	0.35(5)
Co	x	0	0	0	0
	y	0	0	0	0
	z	1/2	1/2	1/2	1/2
	U_{eq}	0.00326(7)	0.00368(6)	0.00499(7)	0.00553(9)
	U_{11}	0.00296(6)	0.00291(5)	0.00393(6)	0.00373(7)
	U_{33}	0.00386(8)	0.00521(7)	0.00710(8)	0.00915(12)
	s.o.f.	1	1	1	1
O	x	0	0	0	0
	y	0	0	0	0
	z	0.23968(6)	0.23727(7)	0.23525(6)	0.23434(9)
	U_{eq}	0.0047(2)	0.0058(1)	0.0073(1)	0.0076(3)
	U_{11}	0.00468(15)	0.00538(16)	0.0065(2)	0.0065(2)
	U_{33}	0.0048(2)	0.0065(2)	0.0088(2)	0.0098(4)
	s.o.f.	1	1	1	1

[a]Displacement parameter conditions are $U_{11} = U_{22} = 2\ U_{12}$ and $U_{13} = U_{23} = 0$, respectively.

other experimental and crystallographic data are summarized in Table 1. Difference-Fourier syntheses using the final atomic parameters showed no significant residual peaks. The final atomic coordinates and displacement parameters are given in Table 2. All calculations were carried out using the Xtal3.4 package program [37].

2.5. Electron density analysis

The electron density analysis of Li_xCoO_2 was performed by the MEM using the present single crystal data with the computer program PRIMA [38]. In the present analysis, the total number of electrons in the unit cell was fixed at $F(000)$ values; 138.00 for $LiCoO_2$, 135.12 for $Li_{0.68}CoO_2$, 133.32 for $Li_{0.48}CoO_2$, and 132.15 for $Li_{0.35}CoO_2$. The unit cell was divided into $64 \times 64 \times 256$ pixels to ensure good spatial resolution. The number of independent reflections used was 250, 252, 256, and 262 for $LiCoO_2$, $Li_{0.68}CoO_2$, $Li_{0.48}CoO_2$, and $Li_{0.35}CoO_2$, respectively, in the range of $\sin\theta/\lambda < 1.3$ Å^{-1}. The reliability factor of the MEM, R_{MEM}, was 2.34% for $LiCoO_2$, 2.57% for $Li_{0.68}CoO_2$, 1.43% for $Li_{0.48}CoO_2$, and 2.00% for $Li_{0.35}CoO_2$. The R_{MEM} is expressed as $R_{MEM} = \Sigma|F_{obs} - F_{MEM}|/\Sigma|F_{obs}|$, where F_{obs} is obtained by the structure refinement and F_{MEM} is the structure factor calculated from the electron density obtained by the MEM. The obtained three-dimensional electron density distributions were visualized with the program VENUS, which was developed by Dilanian and Izumi [39].

3. Results and discussion

3.1. Single-crystal X-ray diffraction

The single-crystal peak profiles of the as-grown $LiCoO_2$ and the electrochemically delithiated Li_xCoO_2 ($x = 0.48$) are shown in Fig. 2. All of the peak profiles for main Bragg reflections indicated the good single crystal quality of not only the as-grown $LiCoO_2$ but also delithiated Li_xCoO_2 crystals. None of these crystals exhibited peak broadening

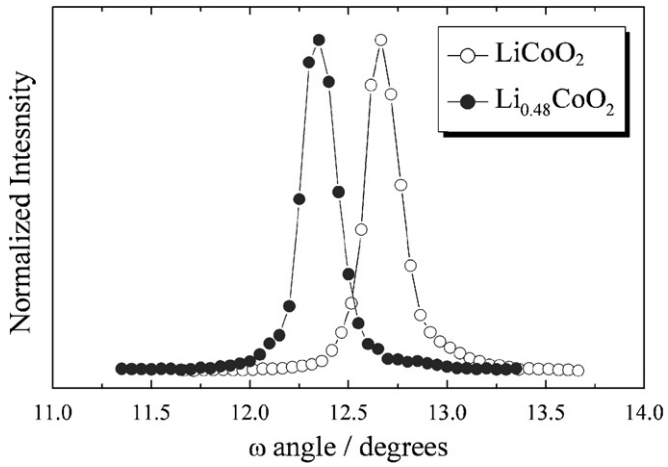

Fig. 2. The single-crystal peak profiles of the 0 0 9 reflection for the as-grown $LiCoO_2$ (open circles) and the electrochemically delithiated $Li_{0.48}CoO_2$ (filled circles) observed on the single-crystal X-ray four-circle diffractometer using Mo$K\alpha$ radiation.

or splitting. The values of full-width at half height for the 0 0 9 reflection were 0.22° for $LiCoO_2$, 0.20° for $Li_{0.68}CoO_2$, 0.22° for $Li_{0.48}CoO_2$, and 0.21° for $Li_{0.35}CoO_2$. From these results, it is possible to say that the single-crystallinity in the delithiated Li_xCoO_2 single crystals remained unchanged in the present experimental conditions, and the phase change upon delithiation was a single-crystal to single-crystal transformation. It is well known that there is a two-phase region corresponding to a voltage plateau at about 3.9 V vs. Li for $0.75<x<0.94$ in Li_xCoO_2 [3–5,7]. The present single-crystal X-ray diffraction study suggests that the two-phase separation reaction could not damage the good single-crystallinity in the Li_xCoO_2 system. We are now investigating the phase separation mechanism in the compositional range of $0.75<x<0.94$ using the chemically delithiated Li_xCoO_2 by the single-crystal X-ray diffraction method.

Precession photographs of Li_xCoO_2 ($x = 0.68$ and 0.35) single crystals indicate that these compounds belong to the trigonal system with the space group of $R\bar{3}m$, which remains unchanged from that of the parent $LiCoO_2$. On the other hand, very weak superlattice spots, e.g., 0 3/2 −3 of the original hexagonal lattice (Fig. 3), were observed in $Li_{0.48}CoO_2$. It is well known that lithium and vacancy ordering in plane leads to a monoclinic distortion for polycrystalline $Li_{0.5}CoO_2$ samples [3,21,22]. However, such a lattice distortion could not be observed in the present $Li_{0.48}CoO_2$ single crystal. All of the superlattice spots can be successfully indexed to $2a \times 2a \times 2c$-type hexagonal lattice ($a = 2 \times 2.8090(15)$ Å and $c = 2 \times 14.3890(17)$ Å) with the same space group of $R\bar{3}m$. However, such a superstructure could not be explained by the above-mentioned lithium/vacancy ordering model in plane. On the other hand, the formation of nano-sized microstructure was reported in the literature [21]. The superlattice structure observed in the present single-crystal study may be explained using a twinned monoclinic lattice with the

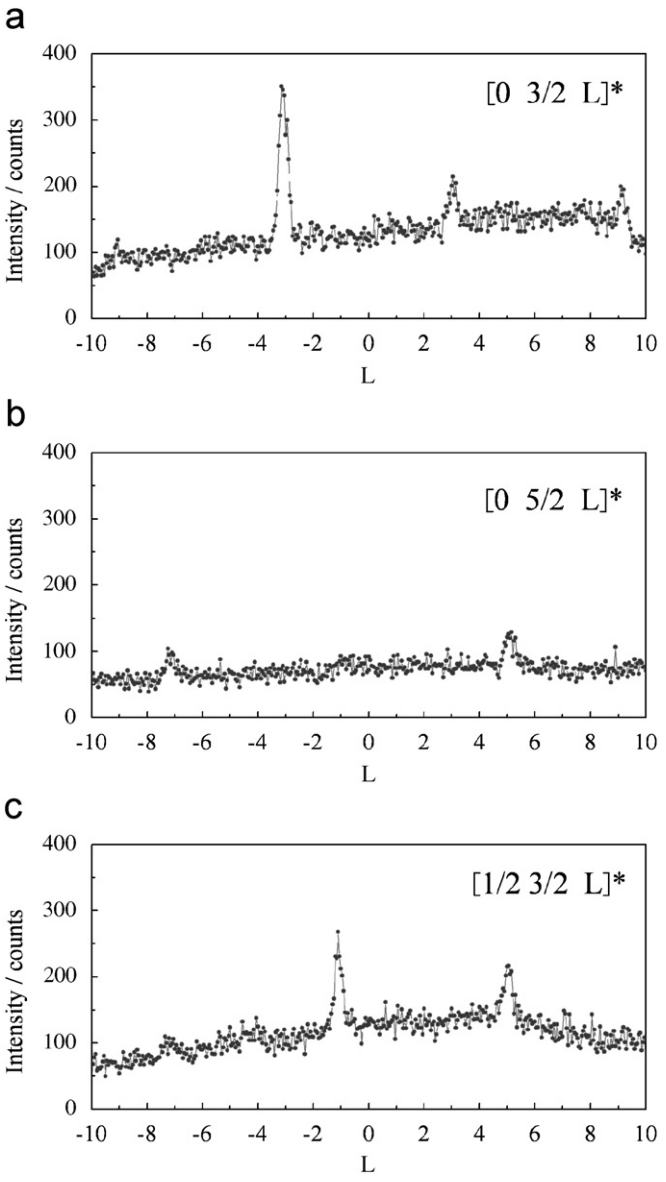

Fig. 3. Diffuse intensity distributions in the electrochemically delithiated $Li_{0.48}CoO_2$ single crystal along (a) the [0 3/2L]*, (b) the [0 5/2L]*, and (c) the [1/2 3/2L]* directions in the range of $-10<L<10$.

space group $P2/m$ [22]: $a = 4.865(3)$ Å, $b = 2.809(3)$ Å, $c = 5.063(3)$ Å, $\beta = 108.68(5)°$, which are identical with that of hexagonal lattice in terms of geometry. In this twin model, all of the superlattice spots can be also indexed to the monoclinic lattice using the twin matrix of: −1/2 −3/2 0/1/2 −1/2 0/1/2 1/2 1. However, the detailed structure analysis failed because the intensity of the observed superlattice reflections was very weak. Accordingly, the average trigonal lattice was chosen for the subsequent structure refinement of $Li_{0.48}CoO_2$.

The refined lattice parameters for the delithiated Li_xCoO_2 are listed in Table 1, in comparison with those for the as-grown $LiCoO_2$. With decreasing lithium content, the c-axis length increased from 14.0542(6) to 14.4359(14) Å, while the a-axis length decreased from 2.8156(6) to 2.8070(12) Å. These values were in good

agreement with the previous results by the power diffraction techniques [3–5,7,8].

3.2. Crystal structure changes upon delithiation

The present structure refinements successfully determined the detailed crystal structure changes upon delithiation for Li_xCoO_2 for the first time. The selected bond distances and angles for $Li_{0.68}CoO_2$, $Li_{0.48}CoO_2$ and $Li_{0.35}CoO_2$ are listed in Table 3, in comparison with the data of as-grown $LiCoO_2$. The basic layered structure of $LiCoO_2$ is maintained in the Li_xCoO_2 compounds with $0.35<x<1$, as shown in Fig. 4. In comparison with the

Table 3
Selected bond distances (Å) and angles (deg) for Li_xCoO_2

	$LiCoO_2$	$Li_{0.68}CoO_2$	$Li_{0.48}CoO_2$	$Li_{0.35}CoO_2$
LiO_6 octahedron				
Li–O	2.0917(6)	2.1214(7)	2.1499(9)	2.1607(10)
O–O	2.8156(6)	2.8107(5)	2.8090(15)	2.8070(12)
O–O′	3.0940(10)	3.1782(12)	3.2553(13)	3.2856(16)
O–Li–O	84.61(2)	82.98(2)	81.58(4)	81.02(3)
O–Li–O′	95.39(2)	97.02(2)	98.42(4)	98.98(3)
CoO_6 octahedron				
Co–O	1.9223(5)	1.9084(6)	1.8985(9)	1.8923(8)
O–O	2.8156(6)	2.8107(5)	2.8090(15)	2.8070(12)
O–O′	2.6180(9)	2.5821(11)	2.5546(12)	2.5385(15)
O–Co–O	94.17(2)	94.85(2)	95.43(4)	95.75(3)
O–Co–O′	85.83(2)	85.15(3)	85.12(4)	84.25(3)

O′ is defined as the oxygen atoms in above and below layers.

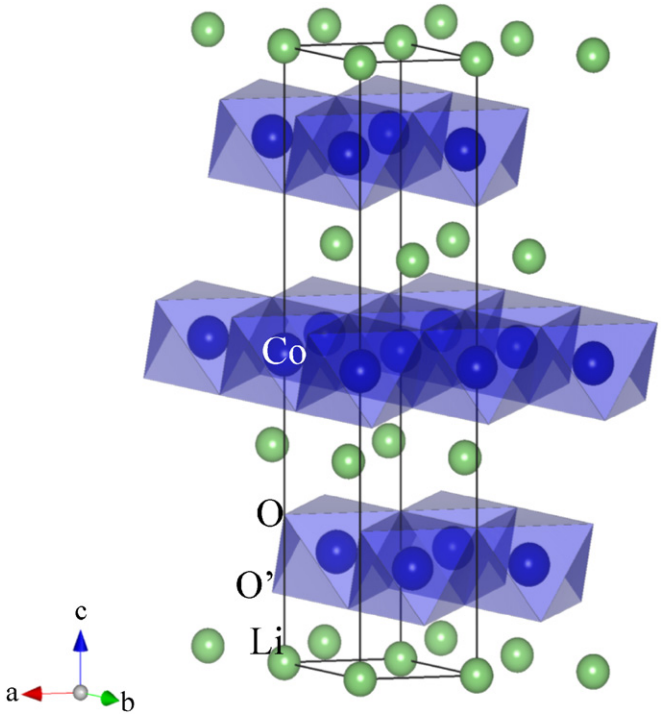

Fig. 4. Crystal structure of $LiCoO_2$. CoO_6 are illustrated as octahedra, and Li atoms as large balls.

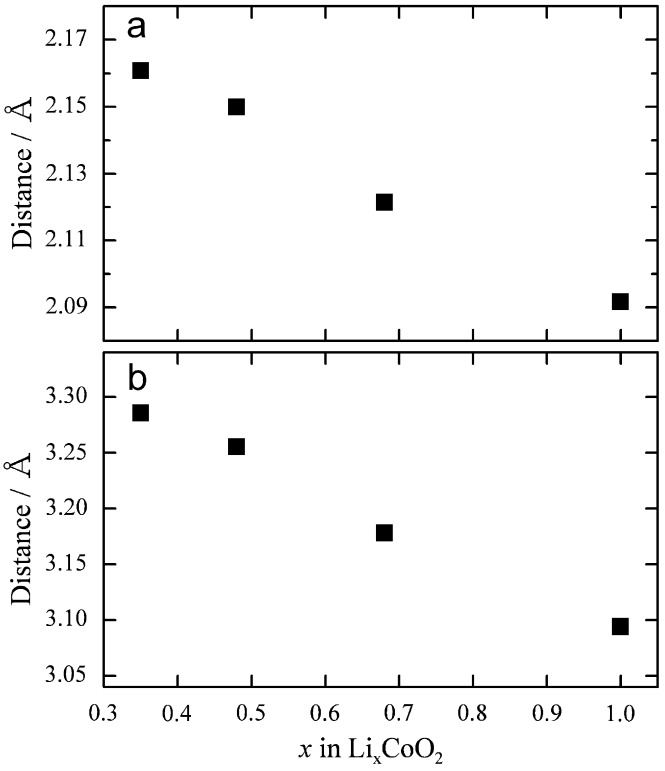

Fig. 5. (a) Li–O and (b) O–O′ distances vs. Li-content in the LiO_6 octahedron of Li_xCoO_2.

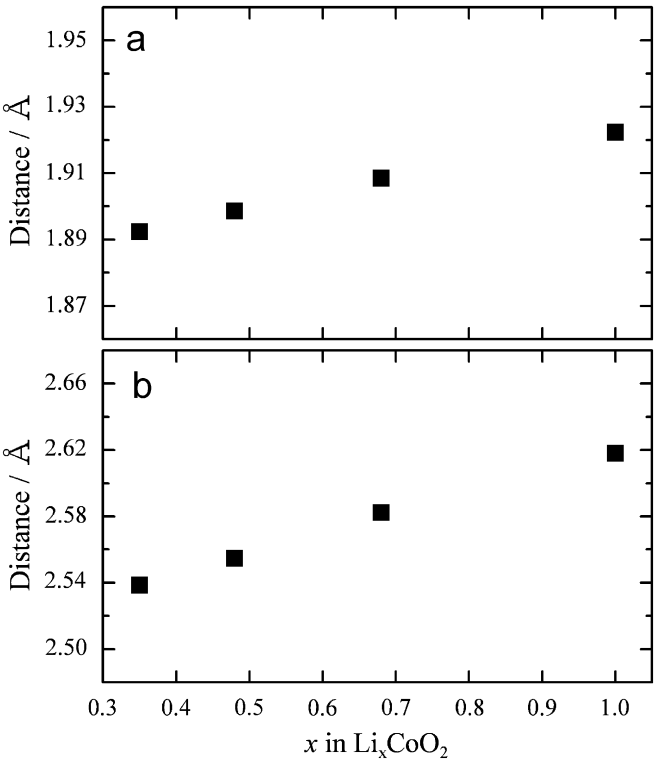

Fig. 6. (a) Co–O and (b) O–O′ distances vs. Li-content in the CoO_6 octahedron of Li_xCoO_2.

structural data of $LiCoO_2$ ($z(O) = 0.23968(6)$), the refined oxygen coordination parameter, $z(O)$, decreases along with decreasing Li-content (Table 2). The negative deviations of the z parameters from the ideal value of 0.25 compress the CoO_6 octahedra and elongate the LiO_6 octahedra.

The octahedral Li–O distance increases together with the Li-deficiency from 2.0917(6) Å in $LiCoO_2$ to 2.1607(10) Å in $Li_{0.35}CoO_2$, as shown in Fig. 5(a). In addition, the O–O′ distance of the LiO_6 octahedron also increases from 3.0940(10) Å in $LiCoO_2$ to 3.2856(16) Å in $Li_{0.35}CoO_2$ (Fig. 5b). These facts indicate an apparent elongation of the LiO_6 octahedron in the c-axis direction. This may have a positive effect on Li-ion diffusion, as previously suggested [19,20]. In fact, along with the decrease in Li-content, the refined anisotropic displacement parameter of U_{11} for the Li atom drastically increased from 0.0126(14) $Å^2$ in $LiCoO_2$ to 0.038(11) $Å^2$ in $Li_{0.35}CoO_2$, while those of U_{33} remained unchanged around 0.009 $Å^2$ in these compounds. The increase in the U_{11} parameters for the Li atom upon delithiation may mean the increase in the thermal displacement of the Li atom in plane from the ideal position.

On the other hand, the Co–O distance of 1.9223(5) Å and the O–O′ distance of 2.6180(9) Å in $LiCoO_2$ were shortened by the delithiation, to the values of 1.8923(8) and 2.5385(15) Å in $Li_{0.35}CoO_2$, respectively (Fig. 6). This short

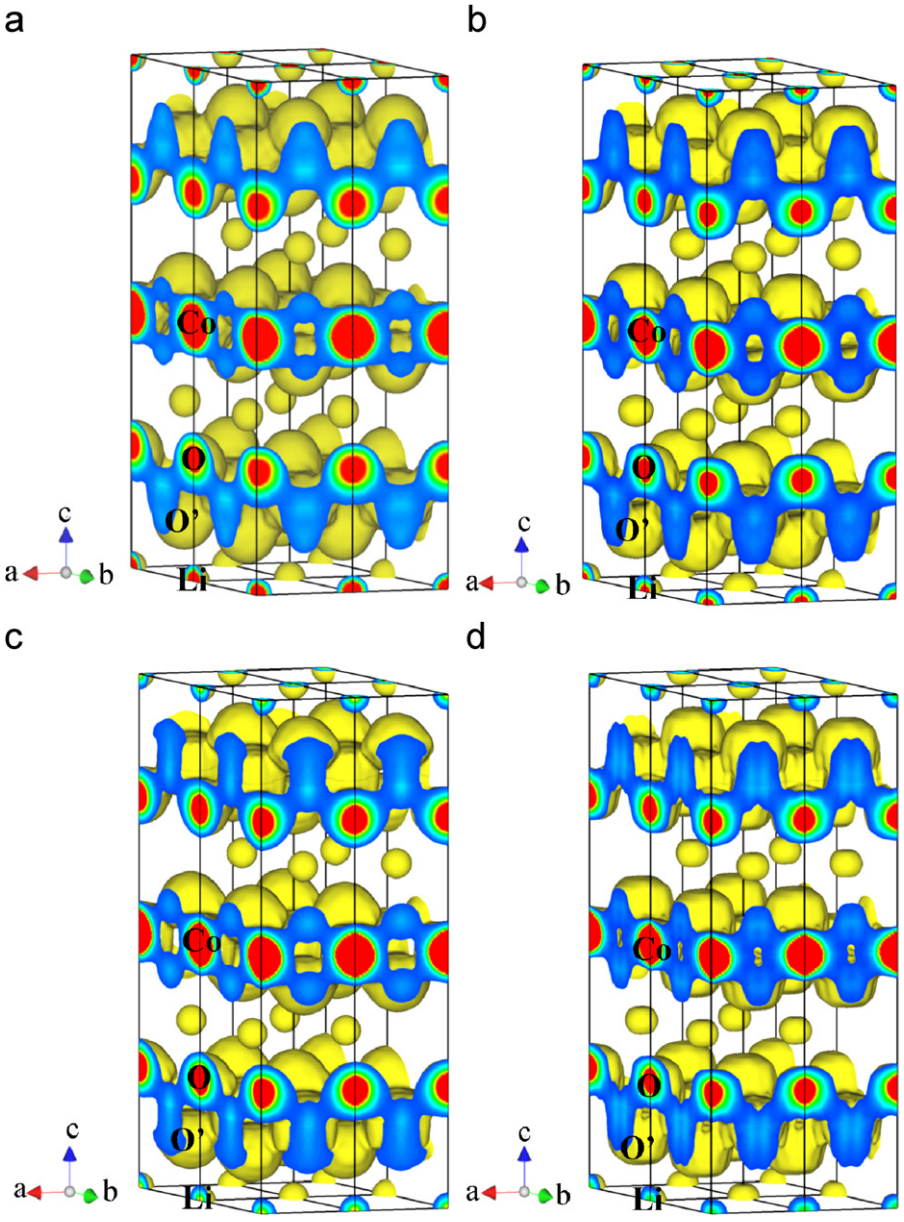

Fig. 7. Three-dimensional electron density distributions of (a) $LiCoO_2$, (b) $Li_{0.68}CoO_2$, (c) $Li_{0.48}CoO_2$, (d) $Li_{0.35}CoO_2$, obtained by the MEM using the computer program PRIMA [38]. These figures were drawn with the program VENUS developed by Dilanian and Izumi [39]. The iso-surface density level colored with light yellow is equal to 0.5 $Å^{-3}$. The density level colored with blue clearly shows the bonding features between atoms, and largest density level colored with red shows position of each atom. The saddle points of the Co–O bonding were situated at the density level colored with blue between the Co and O atoms.

O–O′ distance in $Li_{0.35}CoO_2$ is very similar to those in the metallic $PdCoO_2$ (2.5388 Å) [40] and $Na_{0.74}CoO_2$ (2.5712 Å) [41]. These oxygen–oxygen distances can be well explained using the crystal radius of O^{2-}, the value of which was reported as 1.26 Å [42], because the values are very consistent with $1.26 \times 2 = 2.52$ Å. Accordingly, a further decrease in O–O′ distances upon delithiation in Li_xCoO_2 may suggest the stronger covalency of the Co–O bonds, as previously indicated by XAS and EELS [9–12].

It should be noted that the refined anisotropic displacement parameter of U_{33} for the Co atom increased from 0.00386(8) $Å^2$ in $LiCoO_2$ to 0.00915(12) $Å^2$ in $Li_{0.35}CoO_2$ (Table 2). This fact suggests that the anisotropic character for the Co atom along the *c*-axis direction increases together with the delithiation. A similar anisotropy of the Co atom has been recently reported in $Na_{0.74}CoO_2$ [41]. In addition, the anisotropic displacement parameter of U_{33} for the O atom also increased from 0.0048(2) $Å^2$ in $LiCoO_2$ to 0.0098(4) $Å^2$ in $Li_{0.35}CoO_2$ (Table 2). The anisotropy of displacement parameters for both the Co and O atoms upon delithiation along the *c*-axis direction may be caused by the above-mentioned compression of the CoO_6 octahedra. Namely, the compression results in the decrease of the CoO_6 octahedral volume. Because of the closest O–O and Co–Co atomic arrangements to the in-plane direction, the atomic displacement along the *c*-axis direction from the ideal position for the Co and O atoms may be caused to prevent the layered structure of $LiCoO_2$. In fact, it was previously reported that a further delithiation with $x \sim 0$ in Li_xCoO_2 accompanied the reconstruction of oxygen arrangement from three-layer (O3) to single-layer (O1) phase [5].

3.3. Electron density distribution

Fig. 7 shows the three-dimensional electron density distributions of $LiCoO_2$, $Li_{0.68}CoO_2$, $Li_{0.48}CoO_2$, and $Li_{0.35}CoO_2$ at 300 K obtained by the MEM analysis using the present single-crystal X-ray diffraction data. The iso-surface electron density distributions were visualized with VENUS, the program developed by Dilanian and Izumi [39]. The iso-surface density level is equal to 0.5 $Å^{-3}$. From the MEM analysis in Fig. 7, strong covalent bonding features between the Co and O atoms were clearly visible in all of the Li_xCoO_2 compounds. It was considered that the covalent bonding of Co–O was due to the Co–3*d* and O–2*p* interaction near the Fermi level. The electron density heights at the saddle point between the Co and O atoms were determined to be 0.81 $Å^{-3}$ in $LiCoO_2$, 0.85 $Å^{-3}$ in $Li_{0.68}CoO_2$, 0.75 $Å^{-3}$ in $Li_{0.48}CoO_2$, and 0.81 $Å^{-3}$ in $Li_{0.35}CoO_2$. These values are very similar to those in $NaCoO_2$ (0.78 $Å^{-3}$) [24] and $Na_{0.74}CoO_2$ (0.81 $Å^{-3}$) [41], suggesting the good quality of the analysis in these compounds. Unfortunately, the present electron density analysis could not clearly reveal the valence changes upon delithiation from the viewpoint of bonding electron height at the saddle points. On the other hand, no bonding is observed around the Li atoms in Fig. 7. The iso-surface density distribution at 0.5 $Å^{-3}$ shows a spherical shape, suggesting the ionic character of the Li atom. Fig. 8 shows the changes of the electron density, $\rho(r)$, at the Li site in Li_xCoO_2. It is clearly found that the electron density gradually decreases upon delithiation. Although this decrease is widely assumed to occur, this is the first time it has been experimentally confirmed.

Fig. 9 shows the electron density, ρ(r), and the radial distribution of the electron density, $\sigma(r) = 4\pi r^2\rho(r)$, for the Li, Co, and O sites in $LiCoO_2$. In the radial distribution curves for the Co and O sites, two peaks are clearly observed in the range of $0 < r_{\langle 100 \rangle} < 1$. In the case of the Co site, a sharp peak around 0.15 Å corresponds to the distribution of *K*- and *L*-shell electrons, and a second peak around 0.5 Å corresponds to that of *M*-shell electrons of Co. Similarly, it is considered that the two small humps for the O site around $r = 0.15$ and 0.6 Å are mainly due to *K*- and *L*-shell electrons, respectively. On the other hand,

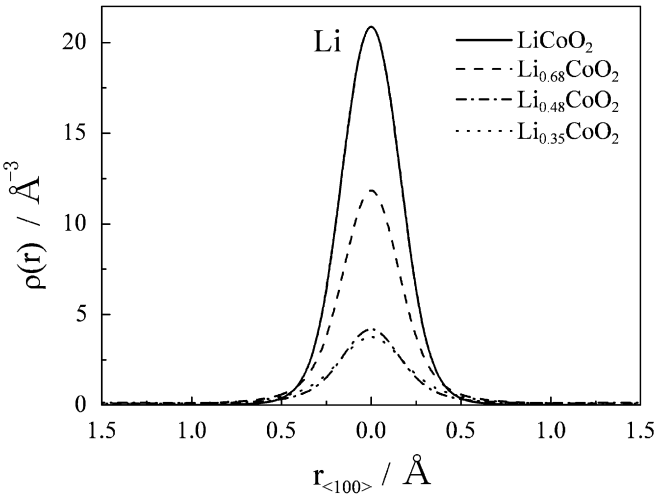

Fig. 8. Changes of the electron density, $\rho(r)$, at the Li site upon delithiation in Li_xCoO_2.

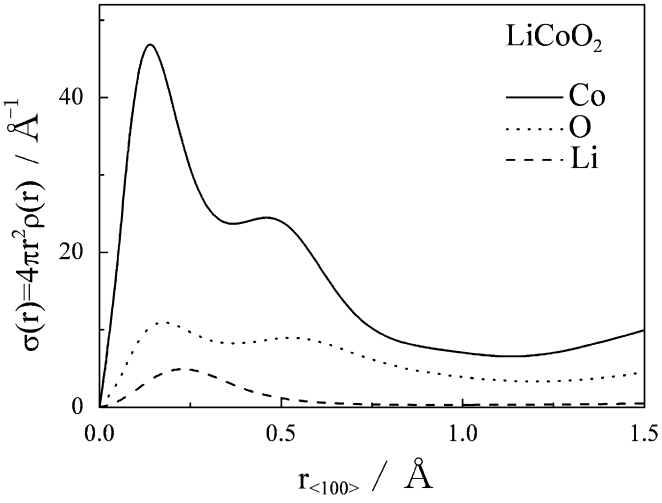

Fig. 9. The electron density, $\rho(r)$, and the radial distribution of the electron density, $\sigma(r) = 4\pi r^2\rho(r)$, for the Li, Co, and O sites in $LiCoO_2$.

there is a small peak around 0.25 Å for the Li site, which is well assigned to two electrons. A further electron density study should be performed in order to precisely determine the net atomic charge of Li_xCoO_2. It will be necessary to improve both the quality of the experimental data and the analytical technique in order to gain a detailed understanding of the nature of the chemical bonding in Li_xCoO_2.

4. Conclusion

We prepared lithium-deficient Li_xCoO_2 single crystals with $x = 0.68$, 0.48, and 0.35 by means of electrochemical and chemical delithiation techniques for the first time. The structure refinement by the single-crystal X-ray diffraction method revealed the precise structural changes upon delithiation. Previously, the abnormally short oxygen–oxygen contact distance of 2.614(2) Å in the CoO_6 octahedron has been emphasized in the structure refinement of $LiCoO_2$ [26]. Upon delithiation, the corresponding O–O′ distance has been revealed to be further shortened to 2.5385(15) Å in $Li_{0.35}CoO_2$. The electron density distributions of these Li_xCoO_2 crystals were analyzed by the MEM using the present single-crystal X-ray diffraction data at 300 K. From the results of the single-crystal MEM, strong covalent bonding was clearly visible between the Co and O atoms, while no bonding was found around the Li atoms in these compounds. We believe that precise electron density analysis is a key to understanding the advantageous characteristics of the charge–discharge cycles in the $LiCoO_2$ electrodes for battery use.

References

[1] K. Mizushima, P.C. Jones, P.J. Wiseman, J.B. Goodenough, Mater. Res. Bull. 15 (1980) 783–789.
[2] S. Kikkawa, S. Miyazaki, M. Koizumi, J. Solid State Chem. 62 (1986) 35–39.
[3] J.N. Reimers, J.R. Dahn, J. Electrochem. Soc. 139 (1992) 2091–2097.
[4] T. Ohzuku, A. Ueda, J. Electrochem. Soc. 141 (1994) 2972–2977.
[5] G.G. Amatucci, J.M. Tarascon, L.C. Klein, J. Electrochem. Soc. 143 (1996) 1114–1123.
[6] R. Gupta, A. Manthiram, J. Solid State Chem. 121 (1996) 483–491.
[7] M. Ménétrier, I. Saadoune, S. Levasseur, C. Delmas, J. Mater. Chem. 9 (1999) 1135–1140.
[8] N. Imanishi, M. Fujiyoshi, Y. Takeda, O. Yamamoto, M. Tabuchi, Solid State Ionics 118 (1999) 121–128.
[9] L.A. Montoro, M. Abbate, J.M. Rosolen, Electrochem. Solid State Lett. 3 (2000) 410–412.
[10] Y. Uchimoto, H. Sawada, T. Yao, J. Synchrotron Radiat. 8 (2001) 872–873.
[11] W.S. Yoon, K.B. Kim, M.G. Kim, M.K. Lee, H.J. Shin, J.M. Lee, J.-S. Lee, C.H. Yo, J. Phys. Chem. B 106 (2002) 2526–2532.
[12] J. Graetz, A. Hightower, C.C. Ahn, R. Yazami, P. Rez, B. Fultz, J. Phys. Chem. B 106 (2002) 1286–1289.
[13] Y.I. Jang, B.J. Neudecker, N.J. Dudney, Electrochem. Solid State Lett. 4 (2001) A74–A77.
[14] M.K. Aydinol, A.F. Kohan, G. Ceder, K. Cho, J. Joannopoulos, Phys. Rev. B 56 (1997) 1354–1365.
[15] C. Wolverton, A. Zunger, Phys. Rev. B 57 (1998) 2242–2252.
[16] C. Wolverton, A. Zunger, Phys. Rev. Lett. 81 (1998) 606–609.
[17] A. Van der Ven, M.K. Aydinol, G. Ceder, G. Kresse, J. Hafner, Phys. Rev. B 58 (1998) 2975–2987.
[18] C.A. Marianetti, G. Kotliar, G. Ceder, Nat. Mater. 3 (2004) 627–631.
[19] M. Nishizawa, S. Yamamura, T. Itoh, I. Uchida, Chem. Commun. (1998) 1631–1632.
[20] Y. Iriyama, M. Inaba, T. Abe, Z. Ogumi, J. Power Sources 94 (2001) 175–182.
[21] Y. Shao-Horn, S. Levasseur, F. Weill, C. Delmas, J. Electrochem. Soc. 150 (2003) A366–A373.
[22] M. Catti, Phys. Rev. B 61 (2000) 1795–1803.
[23] M. Sakata, M. Sato, Acta Crystallogr. Sect. A 46 (1990) 263–270.
[24] Y. Takahashi, Y. Gotoh, J. Akimoto, J. Solid State Chem. 172 (2003) 22–26.
[25] Y. Takahashi, J. Akimoto, Y. Gotoh, K. Dokko, M. Nishizawa, I. Uchida, J. Phys. Soc. Jpn. 72 (2003) 1483–1490.
[26] J. Akimoto, Y. Gotoh, Y. Oosawa, J. Solid State Chem. 141 (1998) 298–302.
[27] Y. Takahashi, Y. Gotoh, J. Akimoto, S. Mizuta, K. Tokiwa, T. Watanabe, J. Solid State Chem. 164 (2002) 1–4.
[28] J. Akimoto, Y. Takahashi, Y. Gotoh, S. Mizuta, in: G.A. Nazri, M.M. Thackeray, T. Ohzuku (Eds.), Intercalation Compounds for Battery Materials PV99-24, The Electrochemical Society, Inc., USA, 2000, p. 81.
[29] S. Levasseur, M. Ménétrier, E. Suard, C. Delmas, Solid State Ionics 128 (2000) 11–24.
[30] N. Imanishi, M. Fujii, A. Hirano, Y. Takeda, M. Inaba, Z. Ogumi, Solid State Ionics 140 (2001) 45–53.
[31] S. Levasseur, M. Ménétrier, Y. Shao-Horn, L. Gautier, A. Audemer, G. Demazeau, A. Largeteau, C. Delmas, Chem. Mater. 15 (2003) 348–354.
[32] I. Uchida, H. Fujiyoshi, S. Waki, J. Power Sources 68 (1997) 139–144.
[33] M. Nishizawa, I. Uchida, Electrochim. Acta 44 (1999) 3629–3637.
[34] K. Dokko, M. Nishizawa, M. Mohamedi, M. Umeda, I. Uchida, J. Akimoto, Y. Takahashi, Y. Gotoh, S. Mizuta, Electrochem. Solid-State Lett. 4 (2001) A151–A153.
[35] J. Akimoto, Y. Takahashi, Y. Gotoh, K. Kawaguchi, K. Dokko, I. Uchida, Chem. Mater. 15 (2003) 2984–2990.
[36] R.G. Delaplane, J.A. Ibers, J.R. Ferraro, J.J. Rush, J. Chem. Phys. 50 (1969) 1920–1927.
[37] S.R. Hall, G.S.D. King, J.M. Stewart (Eds.), Xtal3.4 User's Manual, University of Western Australia, Australia, 1995.
[38] F. Izumi, R.A. Dilanian, Recent Research Developments in Physics, vol. 3, Transworld Research Network, Trivandrum, India, 2002, p. 699.
[39] F. Izumi, R.A. Dilanian, Commission on Powder Diffraction Newsletter. No. 32, International Union of Crystallography, USA, 2005, p. 59.
[40] C.T. Prewitt, R.D. Shannon, D.B. Rogers, Inorg. Chem. 10 (1971) 719–723.
[41] Y. Takahashi, J. Akimoto, N. Kijima, Y. Gotoh, Solid State Ionics 172 (2004) 505–508.
[42] R.D. Shannon, Acta Crystallogr. Sect. A 32 (1976) 751–767.